A Comparison of 2D and 3D IP from Copper Hill NSW

Derek Webb
MIM Exploration Australia
dlwebb@mim.com.au

Peter Rowston
MIM Exploration Australia
parowsto@mim.com.au

Gerard McNeill
GPX Geophysical Exploration Services, Australia
gerard@gpx.com.au

SUMMARY

This paper compares the results from 2D inversion of 2D data, 3D inversion of 2D data and 3D inversion of 3D data from a 3D pole-dipole MIMDAS IP survey conducted near Copper Hill NSW.

Six 1.5km lines were laid out over the area of interest at 200m spacings. Data were collected using 'pole-dipole' geometry with 100m dipoles. All receiver stations on all lines were read simultaneously for each transmitter station.

Data were processed using standard (proprietary) MIMDAS processing. 2D data were inverted using UBC's dcip2d software while 2D and 3D data were inverted using UBC's dcip3d code ported to an NEC SX-5 supercomputer. For the 3D models, resistivities were determined by inversion of primary voltages while secondary voltages, after Time Domain Cole-Cole Inversion, were inverted for the IP model. All errors were based linearly upon observational errors.

Results highlight the differences between inversion models for the two datasets. In particular, the models demonstrate the greater resolution of the 3D survey and the restricted ability of 2D surveys to define boundaries subparallel to the survey lines is emphasized.

Keywords : MIMDAS IP, Copper Hill, 3D IP, 3D inversion, 2D inversion, structure.

INTRODUCTION

Copper Hill is located approximately 5km north of Molong in central New South Wales (Figure 1). The main Copper Hill prospect has been described previously (eg Chivas and Nutter, 1975; Morrison, 1998) and very neatly summarised in Denne et al. (2001). A feature of the Copper Hill system is the strong structural control on alteration and sulphide distribution. Denne et al. (2001) also showed that 3D inversion of 2D IP was useful in helping to resolve the structurally complex subsurface geology at the Copper Hill prospect.

The Copper Hill prospect proper has been subject to a significant amount of exploration work in the past including extensive drilling. Away from Copper Hill proper, drilling density declines rapidly with some significant gaps quite close to Copper Hill but still within the overall Copper Hill system. One such area surrounds the Scotch prospect, approximately 800m to the southeast of Copper Hill proper. Encouraging copper-gold mineralisation had been intersected in a drill hole collared to the west of Scotch and in shallower holes 250m to the northwest and southeast. The prospectivity of the zone was tested by a pole-dipole MIMDAS IP/MT survey which was centred approximately on the Scotch prospect.

Given the strong structural control on mineralisation within the Copper Hill system and the diversity of structural orientations, the Scotch area provided a perfect opportunity to assess the merits of a three dimensional (3D) survey. The 3D survey was designed to enable the extraction of standard two dimensional (2D) MIMDAS data. Final data were modelled as 3D inversion of 3D data, 3D inversion of 2D data and 2D inversion of 2D data using the same mesh and relative errors for each inversion. 2D data were inverted using UBC's dcip2d software while 2D and 3D data were inverted using UBC's dcip3d code ported to an NEC SX-5 supercomputer. For the 3D models, resistivities were determined by inversion of primary voltages while secondary voltages, after Time Domain Cole-Cole Inversion, were inverted for the IP model. All errors were based linearly upon observational errors.

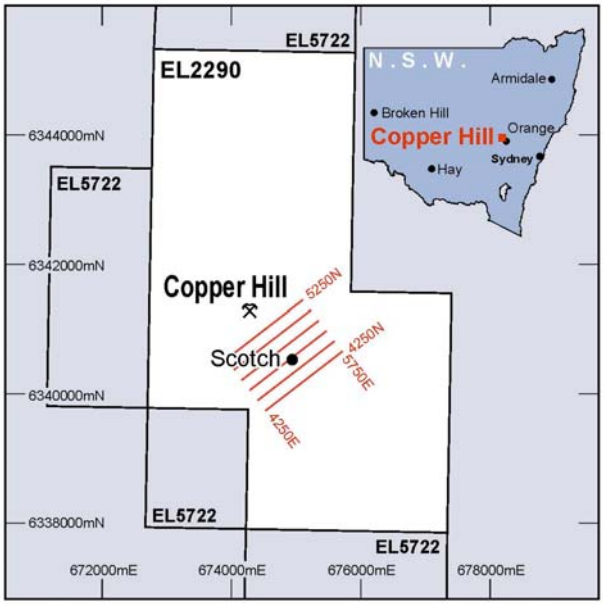

Figure 1. Copper Hill location

Comparison of results for 2D inversion of 2D data, 3D inversion of 2D data and 3D inversion of 3D data was facilitated by 3D visualization and by taking slices through the 3D models and comparing them to the 2D inversion results and each other. Simple observation highlights the greater resolution of the 3D data. This increased resolution is more pronounced at depth. As would be expected, sections through the 3D model for 2D data show improved but similar results to coincident 2D inversions.

METHOD AND RESULTS

Field procedure

A grid consisting of six 1.5 km lines, with 100 metre station spacing and 200 metre separation between lines, was laid out over the area of interest (Figure 2). A pole-dipole survey geometry was used with all six lines set up with receiving dipoles. The centre four lines were set up with the transmitter poles separated by 100 metres and offset by half an a-spacing from the receiver locations to avoid the logistical problems associated with common transmitter and receiver positions.

The six lines of receiving dipoles were set up as a single network allowing them to be read simultaneously for each transmitter pole position. This setup allows true 3D pole-dipole IP data to be collected on all six lines as well as standard 2D pole-dipole IP data to be collected along the four centre lines. It also allows the collection of 200 metre dipole Ey component data which can be used to further constrain the 3D inversion.

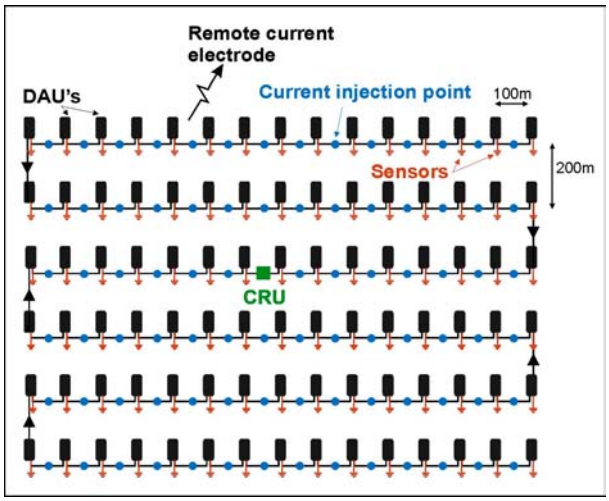

Figure 2. Layout for acquiring 3D IP data at Scotch Prospect, Copper Hill. Data were collected over the entire array for each current injection. DAU's send data back to the CRU via the network at the end of each event. Data path is indicated by black arrows.

The transmitter current was supplied using a 10 kVa system and ranged from 3.0 amps at 800 volts to 9.0 amps at 700 volts. In general, the contact resistances on potential electrode pairs ranged from 100 Ohm to 2.0 kOhm.

The main cultural influences on data were 50Hz power lines, fences, roads and a disused rail line going through the centre of the grid. Considerable effort was put into avoiding coupling of the current wire to the remote electrode with fences and the rail line.

Delays in the acquisition of data were experienced due to inclement weather at the beginning of the survey and continual livestock interference throughout the duration of the survey. In all, six full days were required to set up and acquire the 3D IP data. This also included the acquisition of 3D MT over the grid. (A similar time would be required to acquire 2D data over the six lines.)

The dog box containing the receiver, transmitter and control equipment was set as close to the centre of the grid as possible to ensure the quickest time for data retrieval. The remote transmitter pole was set up at a distance of approximately 7km from the grid centre and almost perpendicular to the grid line orientation.

Controlled source readings were taken using a base frequency of 0.0977Hz (25/256Hz) in an attempt to minimize EM coupling. After the collection of trial time series data at 100, 200 and 400 samples per second, it was decided that time series data would be acquired using a sampling rate of 200 samples per second as this facilitated the efficient collection of good quality data. A minimum of 3 repeat readings of 13 stacks, at 2 periods per stack was taken for each transmitter pole location

Initial processing of the data consists of deconvolving the received waveform from the transmitted waveform and stacking the resulting time domain decays to produce a two period stacked waveform. From this stacked waveform the chargeability is calculated over a given time window, in this case 1.8 to 2.4 seconds. The repeatability of this calculated time domain chargeability was used, along with peak voltage and the frequency domain three point decoupled phase, to determine the data quality.

In general, repeatability was good with the majority of readings requiring the minimum of three stacks to be taken. During each IP reading data were collected and processed for 86 points (number of receiver stations). The majority of three reading sets returned good data for all 86 points.

Real time pseudo-sections of the two dimensional pole-dipole IP data collected on the central four lines could be easily produced in the field. These 2D resistivity and chargeability pseudo-sections were also a good indication of the data quality. 3D resistivity is not easy to calculate in field.

Data Processing

MIMDAS IP surveys are typically run with a 100% duty cycle square wave transmission. This waveform is recorded with the same accuracy and resolution as the received waveform. The timing of sampling between individual distributed acquisition units (DAUs) in any array is of sufficient accuracy to allow the convolution of a desired waveform with the system response to produce theoretical decays. We typically choose a 50% duty cycle idealised waveform and derive a chargeability (mV/V) based on the MIM chargeability standard. This standard is an estimate of the average decay voltage in a chosen off-time window multiplied by 1000 and divided by the average charge voltage for a half-duty square wave response over the complementary on-time window. There is also a degree of normalisation based upon the application of zero-phase filtering. To summarise the Standard MIMDAS IP processing stream

- Streamed time series collection of transmitted and received signals at 100 - 3200 samples per second.
- Convert raw time series into real units (Volts & Amps) via calibrations for sensors and individual DAUs.

- Stacking of transmitted and received time series, optional number of periods per stack.
- Convert stacked data to frequency domain.
- Calculate the system estimation (H) for individual stacks.
- Selective rejection of outlier system estimation stacks.
- Average system estimation stacks, weighted by observational errors.
- Convolve H with 50% duty cycle frequency response at fundamental period, and convert back to time domain for operator QC display.
- Average repeat events, weighted by observational errors.
- Convolve H with unit 50% duty cycle frequency response at fundamental period.
- Convert to time domain.
- Time Domain MIM Chargeability estimation based upon chosen off-time window
- Spectral IP parameter estimation.

The estimation of spectral parameters is important as the commonly used 2D inversion codes use an IP parameter more akin to intrinsic chargeability than an observed chargeability. In 3D acquisition the recovery of intrinsic chargeability is necessary for 3D Inversion

Spectral IP parameters are estimated by time domain least squares inversion of Cole-Cole forward modelling (see also Rowston et al, 2003). Other spectral models such as the Halverson-Wait can then be derived from the final Cole-Cole model.

Inversion modelling

Final data were modelled as 3D inversion of 3D data (3D3D), 3D inversion of 2D data (2D3D) and 2D inversion of 2D data (2D2D) using the same mesh and relative errors for each inversion. 2D data were inverted using UBC's dcip2d software while 3D inversion models for 2D and 3D data were generated using UBC's dcip3d code ported to an NEC SX-5 supercomputer. For the 3D models, resistivities were determined by inversion of primary voltages while intrinsic chargeabilities, after Time Domain Cole-Cole inversion, were inverted for the IP model. All errors were based linearly upon observational errors. 3D inversion of 2D data also used intrinsic chargeabilities and maintained the same mesh and relative errors as the 3D inversion of 3D data. 2D inversion of 2D data for lines 4450N, 4650N, 4850N, and 5050N used the same mesh and relative errors as the 3D modelling. Care was also taken to ensure that smoothing factors and the chi-factor's were, as far as possible, the same for all inversions.

Comparison of inversion results

A crucial tool for the interpretation of 3D models is 3D visualisation. It is notoriously difficult to successfully portray images from 3D visualisation packages in two dimensions. Hence, discussion here relies on sections taken through the 3D models.

Sections through the 3D models were generated to coincide with 2D lines 4450N, 4650N, 4850N and 5050N. Direct visual comparison of resistivity (Figure 3) and chargeability (Figure 4) reveals some improvement in resolution of structure in 2D3D results over 2D2D. Sections extracted from the model generated from the 3D data show greater resolution than either of the two 2D sourced sections. Some structures that appear as curved features in the 2D2D sections are straight in the 3D3D model. The curved appearance of these features in the 2D2D sections is interpreted to be a function of the dip of the structure and the angle at which the line crosses the structure.

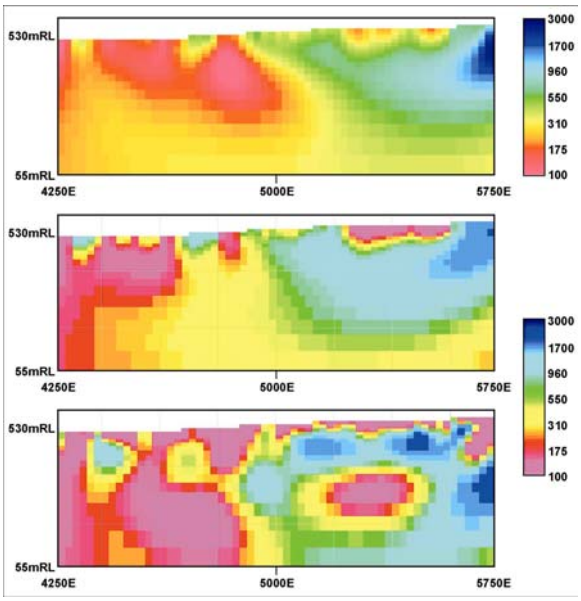

Figure 3. Resistivity model sections for 2D2D (top), 2D3D (centre) and 3D3D (bottom) inversions – Line 4850N.

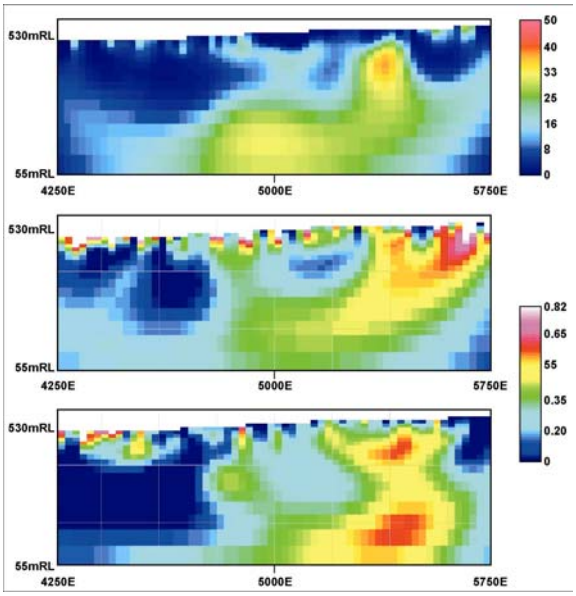

Figure 4. Chargeability model sections for 2D2D (top), 2D3D (centre) and 3D3D (bottom) inversions – Line 4850N. Note that the 2D2D has not detected the moderate east dipping structure in the centre of the section and the poor resolution of a parallel structure (eastern end of sections) in both 2D2D and 2D3D.

2D3D and 3D3D models are compared in both plan and section. In plan (Figure 5), the most obvious difference is in resolution. While the main structural directions (NW, NE, NS) are discernible in both models, they are much more clearly defined in the 3D3D model.

In northing section between survey lines (Figure 6), 3D3D shows even greater improvement in resolution, giving a better representation of the true structural complexity. In particular, east dipping structures are much more clearly defined in the 3D3D model. Note the greater resolution at depth with 3D3D. Similar conclusions can be drawn when comparing easting sections taken through the 3D models. Once again, Figure 7 shows greater resolution for the 3D3D model. 2D3D 'along line' bias can also be seen in this section.

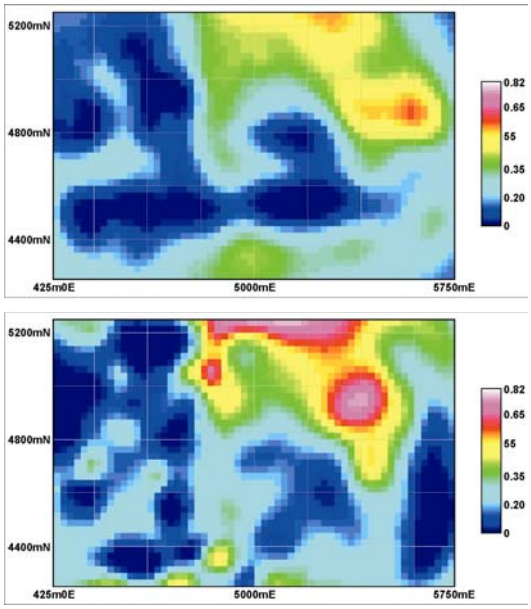

Figure 5. Chargeability model plan sections, 420m RL (80m below lowest point on survey grid) - 2D3D (top) and 3D3D (bottom). Note the significant improvement in resolution of structures for 3D3D.

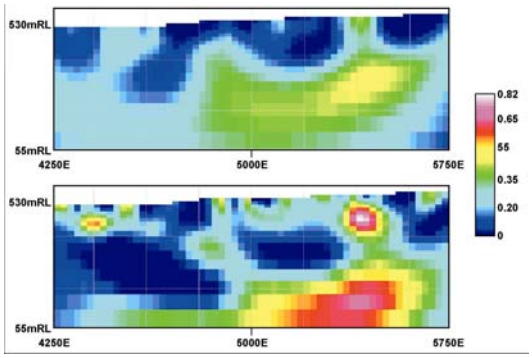

Figure 6. Chargeability model sections for 2D3D (top) and 3D3D (bottom) – 4725N. Note the improvement in resolution for the 3D3D section.

CONCLUSIONS

Comparison of 3D inversion modelling of truly three dimensional IP data and 2D data extracted from the 3D dataset shows that the three dimensional data significantly improves model resolution. 3D models of 2D data do show an improvement over 2D inversions however the 2D data lacks the 'between the lines' information of the truly three dimensional survey which is necessary to properly resolve subsurface geology/ structure. For the MIMDAS system, given that the time required to acquire either 3D or 2D data over the same grid is similar, the extra cost of the 'between the lines' data is effectively the time cost of the extra equipment required.

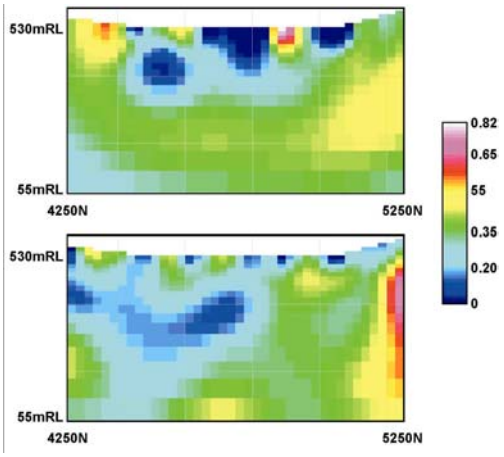

Figure 7. Chargeability model sections for 2D3D (top) and 3D3D (bottom) – 5000E. Note the poor definition of structures in the top section.

ACKNOWLEDGMENTS

The authors would like to thank MIM Exploration Pty Ltd and Golden Cross Resources Ltd for permission to show the data used in this paper. Special thanks to Helen Richmond and Janelle Kuter for their invaluable assistance.

REFERENCES

Chivas, A.R. and Nutter, A.H., 1975, Copper Hill Porphyry Copper Prospect. Knight, S.L. (ed), Economic Geology of Australia and Papua New Guinea vol I. Metals: Australasian Institute of Mining and Metallurgy Monograph No. 5. p 716-720

Denne, R., Collins, S., Brown, P., Hee, R., White, R.M.S, 2001, A New Survey Design for 3D IP Inversion Modelling at Copper Hill: ASEG 15th Conference and Exhibition, Brisbane, Extended Abstracts.

Morrison, G.W., 1998, Copper Hill: Magmatic – Hydrothermal Evolution: Magmatic and Hydrothermal Evolution of Intrusive Relatyed Gold Deposits. AMIRA P425 Final Report.

Oldenburg, D. and Li, Y., 1994, Inversion of induced polarization data: Geophysics 59, 1327-1341.

Rowston, P., Busuttil, S., and McNeill, G., 2003, Cole-Cole Inversion of Telluric Cancelled IP Data: This volume.